International Journal of Pharmaceutics 416 (2011) 171–180

Contents lists available at ScienceDirect

International Journal of Pharmaceutics

journal homepage: www.elsevier.com/locate/ijpharm

# Bivalent sequential binding of docetaxel to methyl-β-cyclodextrin

Silvia Mazzaferro[a,*], Kawthar Bouchemal[a], Jean-François Gallard[b], Bogdan I. Iorga[b], Monique Cheron[a], Claire Gueutin[a], Claire Steinmesse[a], Gilles Ponchel[a]

[a] Univ Paris-Sud, CNRS UMR 8612, School of Pharmacy, 5, Rue J.B. Clément, 92296 Chatenay-Malabry, France
[b] Institut de Chimie des Substances Naturelles, CNRS UPR 2301, Centre de Recherche de Gif-sur-Yvette, 1 Avenue de la Terrasse, 91198 Gif-sur-Yvette, France

ARTICLE INFO

*Article history:*
Received 23 March 2011
Received in revised form 20 June 2011
Accepted 20 June 2011
Available online 25 June 2011

*Keywords:*
Anticancer drug
Docetaxel
Cyclodextrins
Isothermal titration calorimetry
Complexation thermodynamics
Solubilisation studies
Sequential binding
Molecular docking

ABSTRACT

New docetaxel (Dtx) and cyclodextrin (CD) inclusion complexes having improved apparent water solubility (up to 9.98 mg mL$^{-1}$) were obtained from phase solubility diagrams. γ-CD and SBE-β-CD offered only poor solubility enhancements while considerable increases in apparent solubility were obtained with Me-β-CD (20%, w/w) and HP-β-CD (40%, w/w) (9.98 mg mL$^{-1}$ and 7.43 mg mL$^{-1}$, respectively). The complexation mechanism between Dtx and Me-β-CD was investigated by circular dichroism spectrometry, two-dimensional $^1$H NMR (NOESY) in $D_2O$, isothermal titration calorimetry (ITC) and molecular docking calculations. Circular dichroism and NOESY confirmed the existence of non-covalent interactions between Dtx and Me-β-CD and suggested that the *tert*-butyl group ($C_6$–$C_9$) and two aromatic groups ($C_{24}$–$C_{29}$ and $C_{30}$–$C_{35}$) of Dtx interacted with the Me-β-CD molecules. The combination of ITC results to molecular docking calculations led to the identification of an unconventional sequential binding mechanism between Me-β-CD and Dtx. In this sequential binding, a Me-β-CD molecule first interacted with both *tert*-butyl and $C_{30}$–$C_{35}$ aromatic groups ($K_1$: 744 M$^{-1}$). Then a second Me-β-CD molecule interacted with the $C_{24}$–$C_{29}$ aromatic group ($K_2$: 202 M$^{-1}$). The entropy of the first interaction was positive, whereas a negative value of entropy was found for the second interaction. The opposite behavior observed for these two sites was explained by differences in the hydrophobic contact surface and functional group flexibility.



## 1. Introduction

Docetaxel (Dtx) is a potent anti-cancer drug that displays a broad spectrum of antitumor activity (Engels and Verweij, 2005) being used in clinical trials for the treatment of prostate and breast cancers as well as lung carcinoma. Dtx is a very sparingly water-soluble drug (0.0019 mg mL$^{-1}$) making difficult to formulate it efficiently. Dtx is currently administered by the parenteral route and is commercially formulated as a solution containing polysorbate 80 which causes severe allergic reactions and peripheral neuropathology (Nuijen et al., 2001). In clinical practice, the incidence of these severe hypersensitivity reactions requires the oral administration of dexamethasone and antihistamine before Dtx infusion. Thus, the search for alternative routes of administration is of practical importance when looking for suitable formulations either for parenteral or oral delivery. For parenteral delivery, the increase in the apparent solubility of Dtx should be looked for using acceptable excipients. When foreseeing oral delivery, it should be remarked that Dtx belongs to the Class IV of the Biopharmaceutical Classification System, which comprises substances with both low solubility in aqueous fluids and low apparent permeability. These substances are substrates of biological transporters and/or metabolized in the intestinal barrier. In this situation, improving the apparent solubility of such substances may solve only one aspect of the problem but is obviously requested as a starting point for the design of efficient pharmaceutical formulations. In this context, one strategy to improve Dtx solubility is to use cyclodextrins (CDs). Complexation of poorly water-soluble drugs with natural or chemically modified CDs represents an interesting strategy for increasing their apparent water solubility (For reviews see Brewster and Loftsson, 2007; Del Valle, 2004; Duchêne et al., 1999; Loftsson and Duchêne, 2007; Rajewsky and Stella, 1996) and offers further possibilities for their pharmaceutical formulation ranging from conventional to colloidal dispersions (Agüeros et al., 2009; Bellocq et al., 2003; Bouchemal et al., 2009a,b; Daoud-Mahammed et al., 2009, 2010; Maestrelli et al., 2010; Othman et al., 2009, 2011; for review see Duchêne et al., 1999).

Shaped as a hollow truncated cone, CDs are composed of cyclic oligosaccharides of D-(+) glucopyranose units, all in chair confor-

* Corresponding author at: Univ Paris-Sud, CNRS UMR 8612, « Physico-chemistry, Pharmacotechny & Biopharmacy », School of Pharmacy, 5, Rue J.B. Clément, 92296 Châtenay-Malabry, France. Tel.: +33 01 46 83 57 12; fax: +33 01 46 61 93 34.
*E-mail address:* silvia.mazzaferro@u-psud.fr (S. Mazzaferro).

0378-5173/$ – see front matter © 2011 Elsevier B.V. All rights reserved.
doi:10.1016/j.ijpharm.2011.06.034

mation, linked by α-(1,4) glucosidic bonds. This molecular structure confers to CDs the shape of a truncated cone, with the outer side formed by the secondary 2- and 3-hydroxyl groups and the narrow side by the primary 6-hydroxyl groups. Thanks to this conformation, CDs have lipophilic inner cavities and hydrophilic outer surfaces. Interactions generally occur between CDs and lipophilic molecules or lipophilic groups borne by the molecules, resulting in the formation of inclusion complexes. CD/drug complexes can be much more water-soluble than the non-complexed drug. However, in spite of the numerous advantages of CDs for the improvement of apparent drug solubility, few research works detailed the solubilisation of Dtx by using CDs (Thiele et al., 2010). In the literature most data about the complexation of taxane derivates with CDs concern paclitaxel (Alcaro et al., 2002; Bouquet et al., 2007; Dordunoo and Burt, 1996; Hamada et al., 2006; Kagkadis, 2007; Lee et al., 2001; Liu et al., 2003; Sharma et al., 1995). So far, the investigation of the CD/Dtx molecular interaction has not been reported in the literature yet and remains a fundamental question that needs to be solved.

In the work to be presented here, phase-solubility diagrams were first used to screen the potential of different CDs to enhance aqueous solubility of Dtx and to identify the best CD capable of improving Dtx aqueous solubility. Then, an in depth physicochemical methods including nuclear magnetic resonance ($^1$H NMR) coupled with two-dimensional nuclear overhauser effect (NOESY), isothermal titration calorimetry (ITC) experiments and molecular modeling were used to investigate the mechanism of CD/Dtx complexation.

## 2. Materials and methods

### 2.1. Reagents

Anhydrous docetaxel (Dtx) ($M_w$ = 807.85 g mol$^{-1}$), was purchased from Chemos GmbH (Germany). Random methyl-β-cyclodextrin (Me-β-CD Rameb®, $M_w$ = 1320 g mol$^{-1}$) was purchased from Cyclolab (Budapest, Hungary), hydroxypropyl-β-cyclodextrin (HP-β-CD, $M_w$ = 1309 g mol$^{-1}$) from Acros Organics (Belgium), γ-cyclodextrin (γ-CD, $M_w$ = 1297 g mol$^{-1}$) Cavamax® W8 from ISP (Netherlands) and sulfobutylether-β-cyclodextrin (SBE-β-CD, $M_w$ = 2241 g mol$^{-1}$) Captisol® was a gift from CyDex Pharmaceuticals, Inc. (USA). All chemicals were of analytical or reagent grade and were used without further purification. Solutions were prepared by weight using MilliQ® water (Millipore, France). Analytical grade methanol and ethanol were obtained from Carlo Erba (Italy). Deuterium oxide ($D_2O$) (99.96% D) was obtained from Sigma–Aldrich (Germany) and chloroform-d (99.8% D) from Carlo Erba Reactifs-SDS (France).

### 2.2. Phase solubility diagrams and apparent solubility determinations

Phase-solubility studies were carried out according to the method described by Higuchi and Connor (1965). An excess of commercial Dtx was placed in a glass vial (20 mL) with 2 mL of solubilizing agent which was an aqueous solution of Me-β-, HP-β- or SBE-β-CD at concentrations ranging from 5% to 40% (w/w) and from 5% to 10% (w/w) only for γ-CD, due to solubility limitations.

Vials containing an excess of Dtx powder dispersed in a solution of CD were kept in a shaker for 108 h at 25 °C. This duration was estimated to be long enough for reaching the complexation equilibrium. Then, the samples were filtered through a 0.22 μm membrane filter (Millex, SLAP 0225, Millipore, France).

The solubility of Dtx in water was determined according to the same protocol without the presence of CDs.

### 2.3. Determination of Dtx concentration

After appropriate dilution with HPLC mobile phase, the samples containing Dtx were analyzed by reversed phase HPLC using a symmetry $C_{18}$ column (250 mm × 4.6 mm) and UV detection at 231 nm (Waters system, France). The mobile phase was an isocratic mixture of methanol/water (70:30%, v/v). HPLC analyses were performed at a flow rate of 1 mL min$^{-1}$. Stock solutions of Me-β-CD/Dtx and HP-β-CD/Dtx complexes (400 μg mL$^{-1}$ and 100 μg mL$^{-1}$ respectively) were prepared according to the method described in the previous section. The concentration of Dtx should be below the solubility of the inclusion complex. Both stock solutions were diluted with the mobile phase. Valid concentrations for quantification were in the range 0.5–400 μg mL$^{-1}$ for the Dtx with Me-β-CD, and 0.1–100 μg mL$^{-1}$ for HP-β-CD. The equations of the calibration curves were $y = 59.42(\pm 0.19)x + 62.05(\pm 28.40)$, $r^2 = 0.9999$ and $y = 59.83(\pm 0.32)x + 33.706(\pm 12.41)$, $r^2 = 0.9995$ for Me-β-CD and HP-β-CD, respectively. However, it was not possible to prepare sufficiently concentrated stock solutions of Dtx complexes prepared with SBE-β-CD and γ-CD due to the poor Dtx solubilisation effect obtained when using these two CDs. A Student's *t*-distribution test was carried out to compare the slope and the intercept of the two previous equations. The *p*-values were higher than 5% (28.7% and 36.5% respectively), supporting that the two linear least square lines could be considered statistically equal. For this reason the concentrations of Dtx for SBE-β-CD and γ-CD were estimated from the one obtained with Me-β-CD/Dtx complex.

### 2.4. Circular dichroism spectrometry

Circular dichroism spectra of Me-β-CD/Dtx inclusion complexes were determined by using a Jasco J-810 Circular Dichroism Spectropolarimeter. Me-β-CD/Dtx inclusion complexes were prepared according to the protocol described in Section 2.2 by using a 10% (w/w) Me-β-CD solution. The circular dichroism spectra were recorded in the 200–400 nm wavelength domain at room temperature. Circular dichroism spectrum for Me-β-CD/Dtx inclusion complex was compared to those obtained for Me-β-CD and Dtx separately.

### 2.5. Nuclear magnetic resonance (NMR) experiments

$^1$H NMR spectra were obtained by operating at 300 MHz (Brucker 300 Avance) and 800 MHz (Bruker Avance 3, TCI Cryoprobe) for the free Dtx and at 600 MHz (Bruker Avance, TXI SB 5 mm) for the inclusion complex and the Me-β-CD alone. The two-dimensional nuclear Overhauser effect (NOESY) spectra of the complex were performed with a Bruker Avance, TXI Cryoprobe at 600 MHz.

The inclusion complex of Dtx and Me-β-CD (10%, w/w) was prepared as described in Section 2.2 by replacing water by $D_2O$. Free Dtx solutions were prepared by placing an excess of commercial Dtx powder in a glass vial (20 mL) with either 2 mL of $D_2O$ (for the $^1$H NMR at 800 MHz) or $CDCl_3$ (for the $^1$H NMR 300 MHz). Then, the samples were filtered through a 0.22 μm membrane filter (Millex, SLAP 0225, Millipore, France). Chemical shifts were reported in ppm (δ) downfield from tetramethylsilane (TMS) internal reference.

### 2.6. Isothermal titration calorimetry (ITC) experiments

An isothermal calorimeter (ITC) (MicroCal Inc., USA) with a cell volume of 1.44 mL has been used for determining from a single titration curve simultaneously the enthalpy of the interaction between Dtx and Me-β-CD and when appropriate, equilibrium constant corresponding to the formation of a complex between those species. The ITC instrument was periodically calibrated either elec-

trically using an internal electric heater, or chemically by measuring the dilution enthalpy of methanol in water. This standard reaction was in excellent agreement (1–2%) with MicroCal constructor data.

Typically, aliquots of 5 μL of Me-β-CD solution (10 mM) filled into a 283 μL containing syringe were used to titrate a 0.703 mM Dtx solution placed in the titration cell which was accurately thermostated at 25 °C. The corresponding heat flows were recorded as a function of time. Intervals between injections were 120 s and stirred at 394 rpm. Due to the poor aqueous solubility of Dtx, solutions were obtained by dissolving the Me-β-CD or Dtx into a water/ethanol mixture (1:1, v/v).

Enthalpograms consisting in series of heat flows were collected automatically. Prior to their analysis, a background enthalpogram consisting in a series of injections of a Me-β-CD solution in a water/ethanol 1:1 (v/v) into a water/ethanol 1:1 (v/v) mixture placed in the titration cell was subtracted from each experimental enthalpogram to account for possible dilution effects. The interaction process between the two species has been analyzed by using different models proposed in the Windows-based Origin 7 software package supplied by MicroCal. Based on the concentrations of the titrant and the sample, the software used a nonlinear least-squares algorithm (minimization of Chi2) to fit the series of heat flows to an equilibrium binding equation, providing the best-fit values of the stoichiometry ($N$), binding constant ($K$) and change in enthalpy ($\Delta H$). From these results, the free energy ($\Delta G$) and the entropy ($\Delta S$) were deducted according to the equation:

$$\Delta G = -RT \ln K = \Delta H - T\Delta S.$$

### 2.7. Molecular modeling

To gain insight into the interaction between Dtx and Me-β-CD, molecular modeling was used. The Me-β-CD structure used in this work was generated from the curated coordinates of ligand QKH (structure 2QKH, Parthier et al., 2007), downloaded from HIC-Up database (Kleywegt, 2007), by manually adding methyl groups on all free hydroxyl groups in order to obtain a fully permethylated structure (GaussView 5, Semichem Inc.). All dihedral angles of the methoxy groups were then homogenised, the resulting conformations being compatible with an unhindered CD cavity. The curated 3D coordinates of Dtx (TXL), ligand present in structures 1TUB (Nogales et al., 1998) and 1IA0 (Kikkawa et al., 2001) were also downloaded from HIC-Up database (Kleywegt, 2007) and used without modification.

CD dimers were generated from two identical monomers aligned on the cavities' axes, with the outer sides pointing one to another. As the optimal distance between CD monomers is not known, eleven dimers were generated, with distances between cavities' centers ranging from 10 Å to 20 Å, which were then used as receptors in the docking procedure.

Molecular docking was carried out using Glide (Friesner et al., 2004) within the Schrödinger Molecular Modeling Suite (http://www.schrodinger.com/). The receptor was prepared using the Protein Preparation Workflow, then the grid was calculated centered on cavity center for 1:1 complexes and on half-distance between cavities centers for 2:1 complexes. Standard precision (SP) protocol was used for the docking process, followed by post-docking minimization. All other parameters were used with the default values.

Molecular modeling images were generated using Chimera software (Pettersen et al., 2004) and the PDF3D representation of the 2:1 Me-β-CD/Dtx complex (see the Supplementary Information) was obtained using the CACTVS Chemoinformatics Toolkit (http://www.xemistry.com/).

## 3. Results and discussion

A preliminary screening of the potential of different pharmaceutically acceptable CDs (Me-β-, HP-β-, SBE-β- and γ-CD) for increasing the apparent aqueous solubility of Dtx has been investigated. As shown in Fig. 1a, different phase-solubility diagrams were obtained, depending on the CD used. The examination of the phase solubility diagrams gave an overview of the process of complexation. Higuchi and Connor (1965) classified the phase solubility diagrams into "A" and "B" types. "A" type curves indicate the formation of soluble complex, while "B" types are observed when insoluble complexes are formed. Type "A" diagrams are represented by a linear increase in solubility "$A_L$", or by a linear increase with a positive or negative deviation from linearity "$A_P$" and "$A_N$" respectively. "B" type curves are subdivided into "$B_S$" (complex of limited solubility) and "$B_I$" (insoluble complex) (Fig. 1b).

"A" type curves were experimentally obtained by using γ-, SBE-β- and HP-β-CD (Fig. 1a). A linear increase in Dtx solubility as a function of CD concentration was obtained with the γ-CD (type "$A_L$"). However, the solubility enhancement of Dtx was very poor (from 0.0019 mg mL$^{-1}$ to 0.06 mg mL$^{-1}$) (Table 1) and it was

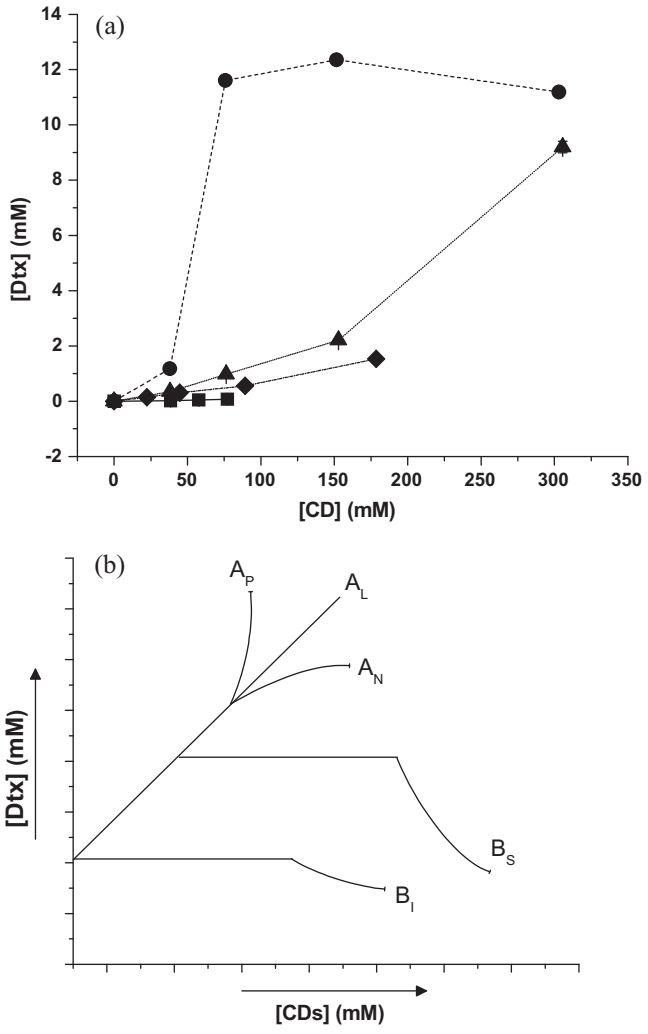


**Fig. 1.** (a) Experimental phase solubility diagram of Dtx for several types of CDs ($n = 3$). (●) Me-β-CD, (▲) HP-β-CD, (♦) SBE-β-CD and (■) γ-CD. (b) Typology of phase solubility diagrams according to Higuchi and Connor (1965), representing: "A": soluble inclusion complex. "B": formation of insoluble inclusion complex. "$A_L$": linear increase of drug solubility as a function of CD concentration. "$A_P$": positively deviated curve. "$A_N$": negatively deviated curve. "$B_s$": complex with limited solubility. "$B_I$": insoluble complex.

**Table 1**
Highest observed apparent solubilities of Dtx in different CD solutions. The apparent solubility enhancement factor (*F*) was obtained by dividing the solubility of Dtx in presence of CDs by the solubility of Dtx in water without CD*. $T^{\circ}$ = 298 K (25 °C), *n* = 3.

| CD | [CD] | | Maximal apparent solubility of Dtx | | *F* |
|---|---|---|---|---|---|
| | (% w/w) | (mM) | (mg mL$^{-1}$) | (mM) | |
| None* | 0 | 0 | 0.0019 | 0.0023 | 1 |
| γ-CD | 10 | 77 | 0.06 ± 0.01 | 0.07 ± 0.01 | 31 |
| SBE-β-CD | 40 | 178 | 1.23 ± 0.01 | 1.53 ± 0.01 | 665 |
| HP-β-CD | 40 | 305 | 7.43 ± 0.17 | 9.20 ± 0.21 | 4000 |
| Me-β-CD | 10 | 75 | 9.38 ± 0.06 | 11.61 ± 0.07 | 4937 |
| | 20 | 151 | 9.98 ± 0.16 | 12.36 ± 0.08 | 5374 |

impossible to increase the concentration of γ-CD above 10% (w/w) because of its own limited water solubility. The SBE-β-CD and the HP-β-CD led to "$A_P$" type curves and the highest Dtx concentration (1.23 mg mL$^{-1}$ and 7.43 mg mL$^{-1}$ respectively) necessitated an important amount of CD (40%, w/w) (Table 1). Interestingly, higher concentrations of Dtx (9.38 and 9.98 mg mL$^{-1}$) were obtained at lower Me-β-CD concentrations (10 and 20%, w/w) compared to SBE-β-CD and HP-β-CD (40%, w/w) (Table 1). This considerable increase in Dtx solubility has never been reported in previous works and may be of interest in formulation practice.

The Me-β-CD diagram could not be assigned to any type and can be divided into four parts: (i) at low Me-β-CD concentration, the diagram should be assigned to $A_L$ type suggesting the formation of 1:1 inclusion complex. (ii) However, at higher concentration of Me-β-CD, the curve positively deviated from linearity suggesting the formation of a 2:1 (Me-β-CD/Dtx) complex (type "$A_P$") (Loftsson et al., 2002). (iii) The solution reached saturation at Me-β-CD concentration above 10% (w/w). (iv) Further increase of Me-β-CD above this concentration had a slight effect on the Dtx apparent aqueous solubility (type "$A_N$"). Finally, for Me-β-CD concentration higher than 20% (w/w) a slight decrease of Dtx solubility was observed (type "$A_N$"). On this basis, Me-β-CD complexes were further characterized. Considering that the concentrations of Dtx with 10% and 20% (w/w) of Me-β-CD were very close (9.38 and 9.98 mg mL$^{-1}$), the lowest concentration of the CD (10%) was preferred for the characterization studies.

Circular dichroism spectroscopy was then used to confirm the existence of interactions between Dtx and Me-β-CD. Circular dichroism spectroscopy is based on the measurement of differences in the absorption of left-handed polarized light versus right-handed polarized light which arises due to structural asymmetry (Daoud-Mahammed et al., 2009; Han and Purdie, 1984). The relatively large increase in signal intensity suggested the existence of interactions between Dtx and Me-β-CD. Fig. 2 presents the circular dichroism spectra of Dtx in the absence or presence of Me-β-CD. Me-β-CD did not show a circular dichroism simply because it does not absorb UV light in the considered wavelength range. On the contrary, Dtx molecules in solution produced a circular dichroism spectrum. A negative circular dichroism band at 280–300 nm was observed. This band was very weak due to the low concentration of Dtx in experimental samples, which was related to the low aqueous solubility of this drug. On the contrary, in the presence of Me-β-CD, the intensity of this band increased, which was due to the enhancement of apparent Dtx aqueous solubility, considering that Me-β-CD did not show any circular dichroism band.

To further investigate the nature of the interactions of Dtx with Me-β-CD, such as the possibility of an inclusion of a Dtx molecule or a specific chemical group within a Me-β-CD cavity, $^1$H NMR and the 2D-NOESY experiments were necessary. A first experiment was carried out by $^1$H NMR in order to compare the spectra of the Me-β-CD/Dtx complex with the one of the free drug and Me-β-CD. It was very difficult to dissolve a sufficient quantity of Dtx in $D_2O$

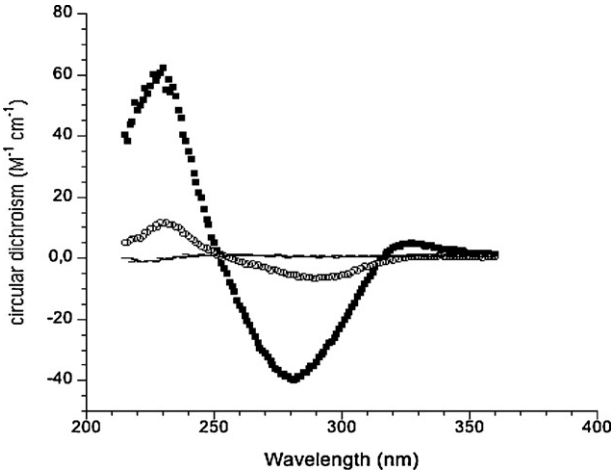


**Fig. 2.** Circular dichroic spectra of free Dtx (0.0019 mg mL$^{-1}$) (○), Me-β-CD (–) (10%, w/w) and their inclusion complex (Me-β-CD/Dtx) (0.75 mg mL$^{-1}$) (■).

necessary to perform the analysis. Considering that Dtx water solubility was 0.0019 mg mL$^{-1}$, only a Spectrometer NMR at 800 MHz equipped with a special probe (cryoprobe) combined to a high number of the scan (512) were able to increase the NMR sensitivity. To ascertain the attribution of the peaks, it was then necessary to compare Dtx spectrum obtained in $D_2O$ by using $^1$H NMR 800 MHz with the one obtained with Dtx dissolved in $CDCl_3$ by using $^1$H NMR 300 MHz. We checked that the chemical shifts characteristic of Dtx molecule (7.00–8.00 ppm) were similar for $CDCl_3$ (Fig. 3a) and $D_2O$ (Fig. 3b). Noteworthy that the chemical shifts obtained with $CDCl_3$ were similar to the ones described by previous research works (Vasu Dev et al., 2006).

A spectrum of the Me-β-CD/Dtx complex was obtained by using $^1$H NMR 600 MHz instead of 800 MHz and by using a usual number of the scans (*n* = 32) because higher concentrations of Dtx could be obtained in $D_2O$ in presence of Me-β-CD. As shown by phase solubility diagrams, the Dtx water solubility was significantly improved by using Me-β-CD at a concentration of 10% (w/w) (Table 1). The spectrum of the Me-β-CD/Dtx is presented in Fig. 3d. The peaks were localized in the range 3.2–5.3 ppm. The inclusion complex spectrum coincided with the sum of the spectra of free Dtx (Fig. 3b) and Me-β-CD (Fig. 3c). Furthermore, in the complex spectrum, it is important to notice the pronounced chemical shift changes in Dtx and Me-β-CD protons typical of the inclusion complex formation.

The chemical groups of Dtx directly involved in the complexation process with Me-β-CD were then investigated using two-dimensional Nuclear Overhauser Effect measurements. Fig. 4 shows the cross peak NOESY bands in the aromatic region (7.2–8.1 ppm) and methyl region (1.0–1.8 ppm). The largest cross peak coincided with the intermolecular interactions between the hydrogen of Dtx ($C_{24}$–$C_{29}$, $C_{30}$–$C_{35}$ and $C_6$–$C_9$) and the internal hydrogens of the Me-β-CD cavity. These interactions could arise only if a Me-β-CD/Dtx complex is formed. These data suggested that the two aromatic rings and the *tert*-butyl group of Dtx were able to interact with Me-β-CD.

The $^1$H NMR results were confirmed by molecular modeling. In the first step, Dtx was docked into the cavity of one Me-β-CD molecule (1:1 stoichiometry), in order to identify all favorable interaction modes. Two clusters of conformers were obtained, each one corresponding to a distinct interaction mode, as shown in Fig. 5. In the first complex (Fig. 5a and b), the *tert*-butyl and the $C_{30}$–$C_{35}$ phenyl groups are positioned in the Me-β-CD cavity, toward the narrow and the outer side, respectively. In the second one, the $C_{24}$–$C_{29}$ phenyl group is positioned exactly in the center of the Me-β-CD cavity (Fig. 6c and d). In both cases, most hydrogen atoms from

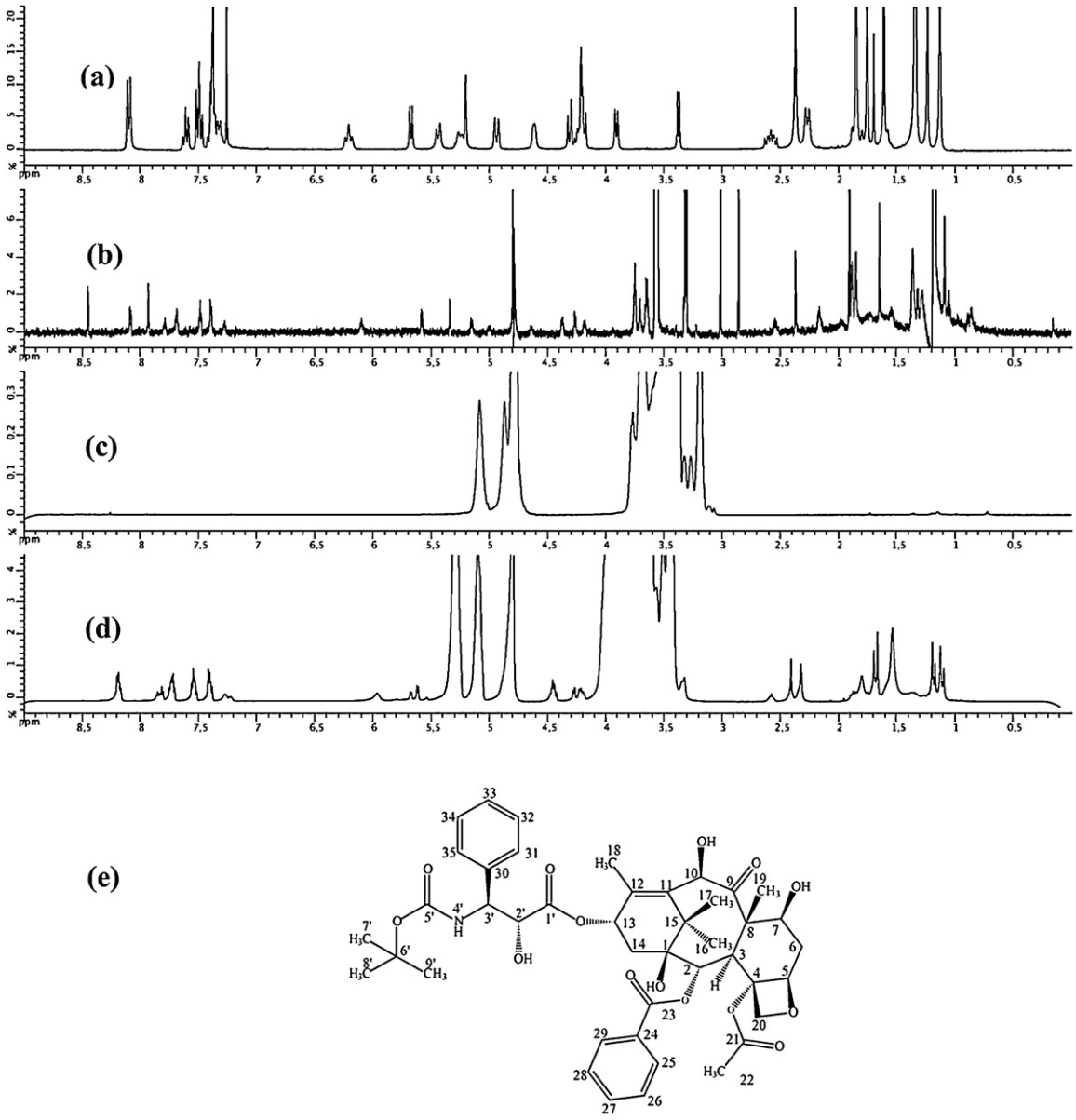


**Fig. 3.** $^{1}$H NMR spectra: (a) free Dtx in $CDCl_3$ (300 MHz, NS = 32, [Dtx] = 10 mg mL$^{-1}$); (b) free Dtx in $D_2O$ (800 MHz, NS = 512, [Dtx] = 0.0019 mg mL$^{-1}$); (c) free Me-β-CD in $D_2O$ (600 MHz, NS = 32, [Me-β-CD] = 10%, w/w); (d) Me-β-CD/Dtx complex (600 MHz, NS = 32, [Dtx] = 5.0 mg mL$^{-1}$) and (e) chemical structure of Dtx.

*tert*-butyl and phenyl groups are in close proximity with the Me-β-CD cavity hydrogen atoms, so these modes of interaction identified by molecular modeling are in full compliance with the NMR data.

In the second step, we wanted to test if it would be possible to form a Me-β-CD/Dtx complex with a 2:1 stoichiometry, an interaction mode with all three hydrophobic groups shielded from solvent contact, while conserving the interacting sites observed in the 1:1 complexes. Thus, cavities of different sizes were generated from two identical Me-β-CD monomers with the outer sides pointing one to another, aligned on the cavities axes, with distances between cavities centers ranging from 10 Å to 20 Å. This orientation is supposed to provide maximum host-guest contact surface and minimum steric hindrance between Me-β-CD monomers. Dtx was then docked into these cavities and the optimum distance between cavities centers was found to be 13 Å. The resulting 2:1 inclusion complex, represented in Fig. 6 (see also Supplementary Information for a PDF3D representation), shows the same Me-β-CD/Dtx interactions as in the 1:1 complexes. Therefore, the complex shown in Fig. 6 can be considered as representative for Me-β-CD/Dtx interaction mode, although an equilibrium between the 2:1 and 1:1 forms cannot be excluded (Davis and Brewster, 2004).

Let us determine now the association constants and the thermodynamic parameters of the interaction between Dtx and Me-β-CD. ITC technique can help to determine whether an association process occurs between two species and allows the evaluation of the association constant ($K$), the stoichiometry ($N$), the enthalpy ($\Delta H$) and the entropy ($\Delta S$) of the Me-β-CD/Dtx interaction from which the Gibbs free energy ($\Delta G$) of the process can be derived (Bouchemal, 2008; Bouchemal et al., 2009b; Kano et al., 2004; Liu et al., 2004; Segura-Sanchez et al., 2009). The enthalpogram corresponding to the interaction between Dtx and Me-β-CD is presented in Fig. 7. Different interaction models available in the ITC apparatus software were tested to fit this enthalpogram, including a one-set of site model, a two-set of sites model and a sequential binding model. The enthalpogram was first fitted to the one-set of site model which describes the interaction with a defined number of identical binding sites. According to the ITC software, the best fit without constraint (i.e. without constraint on the value of the

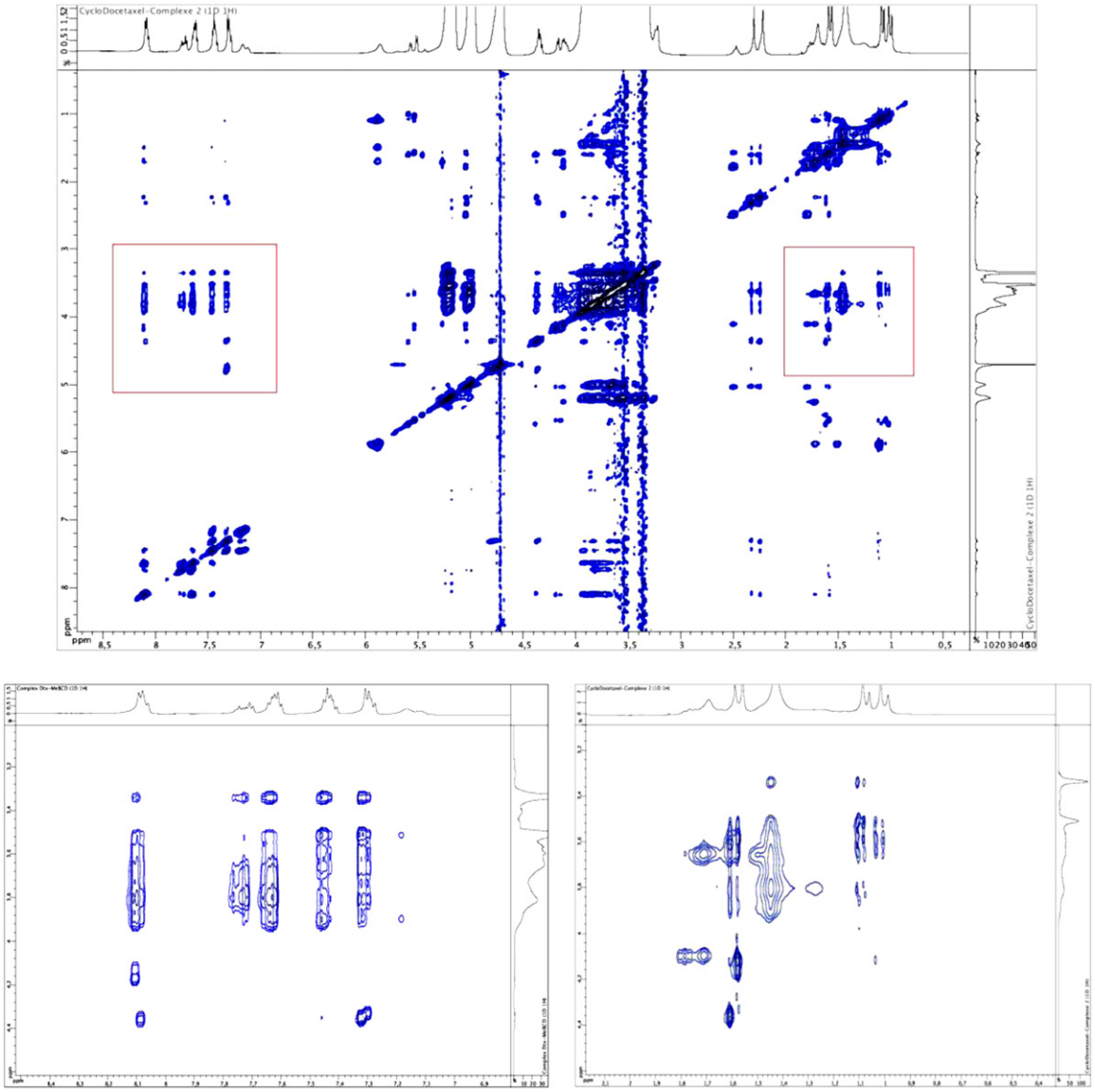

**Fig. 4.** Two-dimensional spectrum of Me-β-CD/Dtx complex (600 MHz, $D_2O$). The largest cross peak coincided with the intermolecular interactions between the hydrogen of Dtx ($C_{24}$–$C_{29}$, $C_{30}$–$C_{35}$ and $C_6$–$C_9$) and the internal hydrogens of the Me-β-CD cavity.

stoichiometry) led to a stoichiometry of the interaction equal to 4 (Table 2), meaning that 4 molecules of Me-β-CD interacted with 1 molecule of Dtx. Obviously, such a stoichiometry would be very unlikely as shown by the molecular modeling which suggested that only two molecules of Me-β-CD were able to interact with one Dtx molecule.

The enthalpogram was then fitted into the same one-set of site model but the stoichiometry of the interaction was imposed and fixed to two CDs for one Dtx molecule. According to this model, the association constant of both interacting groups was 48 $M^{-1}$ and $\Delta H$ was equal to −487 kJ $mol^{-1}$. The value of association constant is too low and the absolute value of $\Delta H$ is too high when compared to the association constants and enthalpies observed for the interaction of β-CD derivatives with molecules bearing *tert*-butyl and aromatic groups. Generally, $K$ is in the range of 130–400 $M^{-1}$ and $\Delta H$ in the range of −10 to 50 kJ $mol^{-1}$(Fini et al., 2004; Segura-Sanchez et al., 2009; Tong et al., 1991; Vasu Dev et al., 2006, for review see Rekharsky and Inoue, 1998).

The one-set of site model considers that all the binding sites are identical as no distinction between the interacting sites is made (Eq. (1)).

$$\text{Dtx} + 2\,\text{Me-β-CD} \overset{K}{\rightleftarrows} \text{Dtx}\cdot(\text{Me-β-CD})_2 \quad (1)$$

However, according to molecular modeling, a Me-β-CD could interact with Dtx according to two distinct modes. The *tert*-butyl and $C_{30}$–$C_{35}$ phenyl groups interacted with one Me-β-CD and the $C_{24}$–$C_{29}$ phenyl group interacted with a second Me-β-CD.

For investigating this possibility, the enthalpogram was then fitted to a two set of sites model. This model yields two distinct binding constants corresponding to the interaction of two Me-β-CDs molecules simultaneously with one Dtx molecule. In this model, association constants are expressed by the following equations:

$$K_1 = \frac{[\text{Dtx}\cdot\text{Me-β-CD}_1]}{[\text{Dtx}][\text{Me-β-CD}_1]} \quad K_2 = \frac{[\text{Dtx}\cdot\text{Me-β-CD}_2]}{[\text{Dtx}][\text{Me-β-CD}_2]} \quad (2)$$

However, this model considers that the two sites are identical and independent, which was unlikely according to molecular modeling and $^1$H NMR (NOESY) results. Finally, a sequential two-

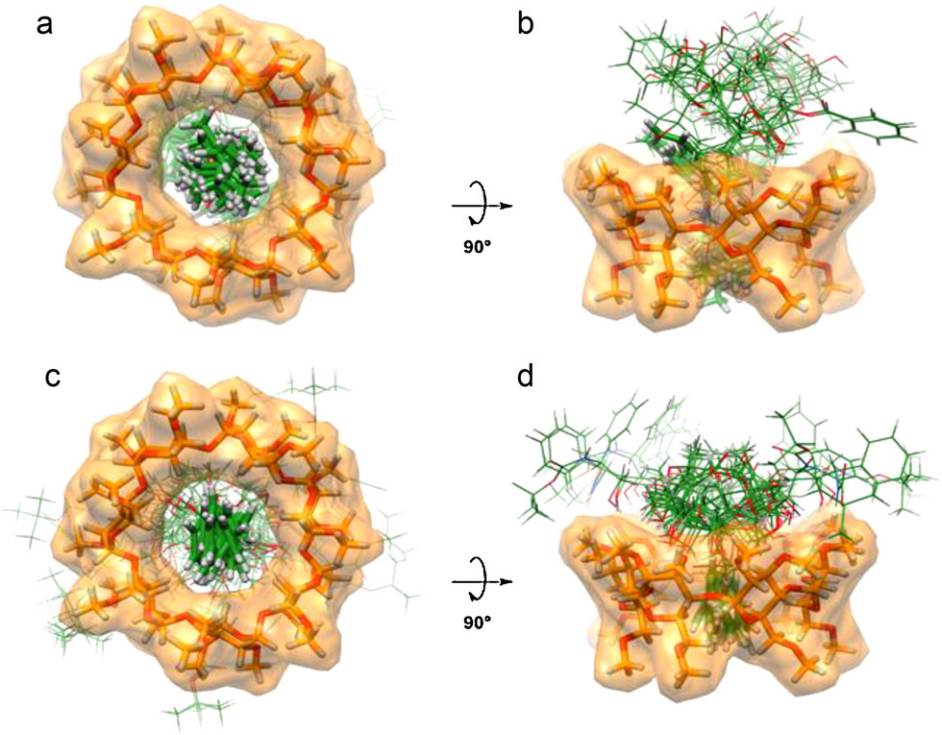


**Fig. 5.** Representation of the two interaction modes (vertical and lateral views) between Me-β-CD (orange) and Dtx (green) obtained by molecular docking (1:1 stoichiometry). The hydrophobic groups interacting with the Me-β-CD cavity are shown in stick representation. (For interpretation of the references to color in this figure legend, the reader is referred to the web version of this article.)

step binding model was found to be more suitable for describing the interactions. This model describes interactions for systems presenting non-identical sites. The two sets of sites model discussed earlier, assumes that the two interactions occur independently one from the other. In the sequential bonding model, the first Me-β-$CD_1$ molecule which binds to Dtx always binds to site 1 (both *tert*-butyl and $C_{30}$–$C_{35}$ aromatic group), then the second Me-β-$CD_2$ molecule which binds to Dtx always binds to site 2 ($C_{24}$–$C_{29}$ aromatic group). Thus, two distinct binding constants are observed but in addition, these binding events are sequential. In this scheme, the Me-β-$CD_1$ molecule would first interact with the Dtx *tert*-butyl and aromatic group ($C_{30}$–$C_{35}$, $K_1$: 744 $M^{-1}$) (Eq. (3)) and then the second Me-β-$CD_2$ molecule would interact with the second aromatic group ($C_{24}$–$C_{29}$, $K_2$: 202 $M^{-1}$) (Eq. (4)). As expected for this type of model, the $\Delta G$ of the second interaction was less negative than the first interaction ($\Delta G_1$: −16.38 kJ $mol^{-1}$ and $\Delta G_2$: −13.15 kJ $mol^{-1}$)

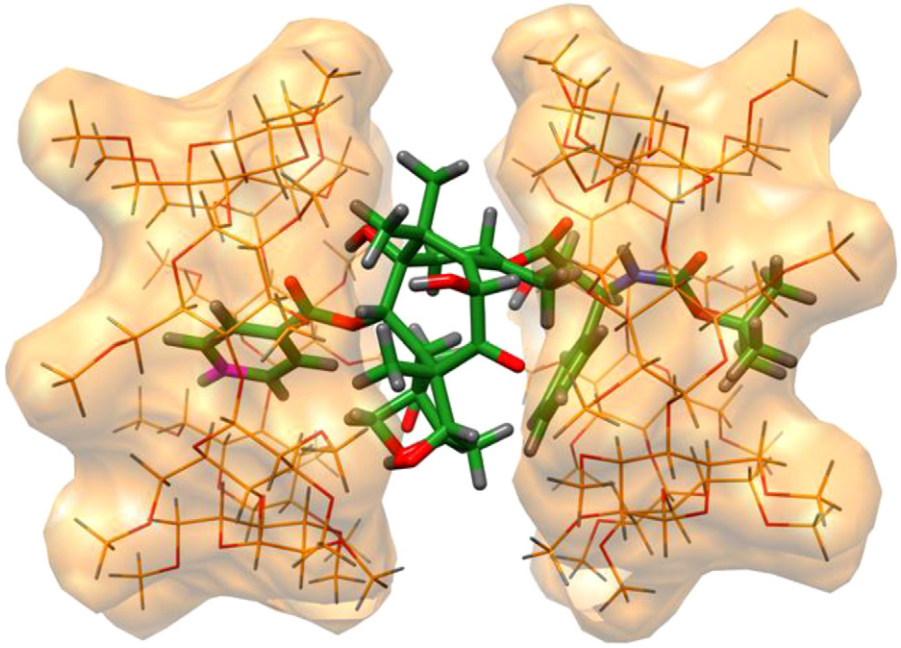

**Fig. 6.** Representation of the complex between Me-β-CD (orange) and Dtx (green) obtained by molecular docking (2:1 stoichiometry). See Supplementary Information for an interactive PDF3D representation of this complex. (For interpretation of the references to color in this figure legend, the reader is referred to the web version of this article.)

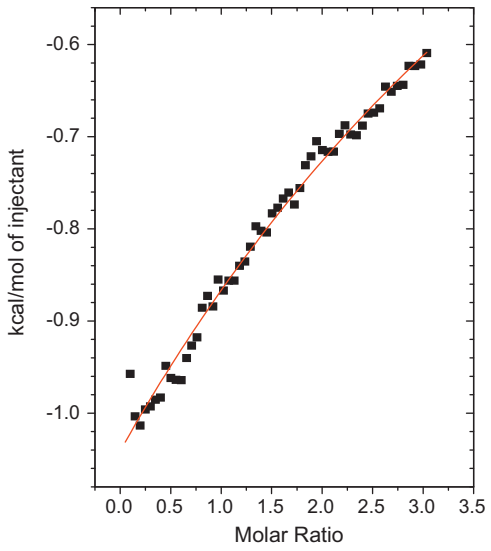


**Fig. 7.** Typical ITC enthalpogram corresponding to the binding interaction developed during the titration of Dtx (0.703 mM) contained in the measurement cell by Me-β-CD (10 mM) contained in the titration syringe at 25 °C giving a differential binding curve which was fit to sequential two-sites binding model yielding the following parameters: $N = 2$, $K_1 = 744\ M^{-1}$, $\Delta H_1 = -12.1\ kJ\ mol^{-1}$, $K_2 = 202\ M^{-1}$, $\Delta H_2 = -27.6\ kJ\ mol^{-1}$.

(Schmidtchen, 2002; Perozzo et al., 2000).

$$Dtx + \text{Me-β-CD}_1 \overset{K_1}{\rightleftarrows} Dtx \cdot \text{Me-β-CD}_1 \quad (3)$$

$$Dtx \cdot \text{Me-β-CD}_1 + \text{Me-β-CD}_2 \overset{K_2}{\rightleftarrows} \text{Me-β-CD}_2 \cdot Dtx \cdot \text{Me-β-CD}_1 \quad (4)$$

$$K_1 = \frac{[Dtx \cdot \text{Me-β-CD}_1]}{[Dtx][\text{Me-β-CD}_1]} \quad K_2 = \frac{[\text{Me-β-CD}_1 \cdot Dtx \cdot \text{Me-β-CD}_2]}{[Dtx \cdot \text{Me-β-CD}_1][\text{Me-β-CD}_2]} \quad (5)$$

The possibility for sequential binding events in CD complexation have been reported for molecules with native CDs, (López-Nicolás et al., 1995; Smith et al., 2009), CD dimers and CD polymers (Liu et al., 2005; Mulder et al., 2004; Xu et al., 2002) but so far, it has never been reported for Dtx and Me-β-CD complexes. The only available association constant for Dtx interaction with β-CD derivates has been experimentally obtained from solubility diagrams (Thiele et al., 2010). A major source of systematic errors lies in the inadequate application of the 1:1 stoichiometry to calculate *K*. Loftsson et al. (2002) have questioned phase solubility diagram method for the determination of association constants. They pointed out that the apparent association constant observed from phase solubility diagrams reflects drug solubilisation by many possible mechanisms other than simple inclusion inside the CD cavities. Indeed, several research groups have shown that CDs may form both inclusion and non-inclusion complexes and that many different types of complexes can coexist in aqueous solutions (Werner and Warner, 1994; Werner et al., 1996). In addition, both CDs and CD/drug complexes are known to form aggregates and it is thought that these aggregates are able to solubilize drugs and other hydrophobic molecules through micellar-type mechanisms (Loftsson et al., 2002; Magnusdottir et al., 2002).

In the present study, the combination of NMR, molecular docking and ITC represented and efficient strategy for evaluating realistic association constants related to the complexation of Dtx with Me-β-CD. Indeed, the superiority of ITC over all other methodologies is the possibility to get deep understanding of the molecular interaction between Dtx and Me-β-CD through the determination of the association constant and thermodynamic parameters. This determination is independent from the solubilisation of the drug since both Dtx and Me-β-CD are in their soluble form. From a thermodynamic point of view, ITC allowed to gain insights into the nature of the non-covalent interactions occurring between Dtx molecule and Me-β-CD leading to the determination of complexation thermodynamic parameters. We demonstrated from molecular docking calculations that no hydrogen bonds were established between Dtx and Me-β-CD in the inclusion complex. The study of $\Delta H$ and $\Delta S$ obtained from ITC data led to the determination of the driving force of the interaction. The interaction is dominated by van der Waals' forces when the process is enthalpy-driven with minor favorable or unfavorable entropies ($|\Delta H| > |T\Delta S|$). However, hydrophobic interactions between two apolar molecules at room temperature have been known as entropy-driven processes, where the entropy of the interaction is large and positive while the enthalpy is small ($|\Delta H| < |T\Delta S|$). For the interaction of Me-β-CD with Dtx, the analysis of thermodynamic data led to the conclusion that the association process was exothermic ($\Delta H < 0$), predominantly driven by enthalpy and moderately by entropy ($|\Delta H| > |T\Delta S|$) for both interacting sites. This thermodynamic signature strongly supports van der Waals-type interactions as the dominant driving force for Dtx complexation with Me-β-CD.

Concerning the entropy, a minor positive entropic contribution ($T\Delta S_1 = 4.27\ kJ\ mol^{-1}$) was observed for the first interaction site (*tert*-butyl and $C_{30}$–$C_{35}$ aromatic groups) and negative entropy for the second interaction site ($C_{24}$–$C_{29}$ aromatic group) ($T\Delta S_2 = -14.47\ kJ\ mol^{-1}$). These thermodynamic behaviors are in accordance with molecular modeling. Positive entropy changes arise from an important flexibility of the interacting species while negative entropy changes usually arise from a significant reduction of the translational and conformational freedoms of host and guest upon complexation (Bouchemal et al., 2009a). The first interaction (Me-β-CD with *tert*-butyl and $C_{30}$–$C_{35}$ aromatic groups) was characterized by a greater hydrophobic contact surface, but also by a flexibility induced by the carbamate linker connecting these two groups, whereas in the second interaction (Me-β-CD with $C_{24}$–$C_{29}$ aromatic group), the interacting groups had a restricted mobility and smaller hydrophobic contact surface, with the phenyl group being kept more tightly in the center of the Me-β-CD cavity. These differences between the two modes of interaction are considered to be responsible for the positive and negative entropic contributions obtained from the analysis of ITC data.

The effect of guest flexibility on association constant and thermodynamic parameters has been reported in many cases and

**Table 2**
Different fitting models leading to the determination of the complex affinity constants (*K*), and thermodynamic parameters corresponding to inclusion complex formation of Dtx (0.703 mM) with Me-β-CD (10 mM) at 298 K (25 °C).

| Fitting model | *N* | *K* ($M^{-1}$) | $\Delta H$ ($kJ\ mol^{-1}$) | $T\Delta S$ ($kJ\ mol^{-1}$) | $\Delta G$ ($kJ\ mol^{-1}$) |
|---|---|---|---|---|---|
| One-site model without constrain on *N* | 4 | 73 | −25.5 | −14.9 | −10.6 |
| One-site model $N = 2$ was imposed | 2 | 48 | −487.6 | −487.0 | −9.5 |
| Two set of sites model | 2 | $K_1$: 130 | $\Delta H_1$: 10.2 | $T\Delta S_1$: 22.3 | $\Delta G_1$: −12.0 |
| | | $K_2$: 73 | $\Delta H_2$: −113.4 | $T\Delta S_2$: −102.8 | $\Delta G_2$: −10.6 |
| Sequential two-binding sites model | 2 | $K_1$: 744 | $\Delta H_1$: −12.1 | $T\Delta S_1$: 4.2 | $\Delta G_1$: −16.3 |
| | | $K_2$: 202 | $\Delta H_2$: −27.6 | $T\Delta S_2$: −14.4 | $\Delta G_2$: −13.1 |

reviewed by Rekharsky and Inoue in their review (1998). They reported that unsaturated compounds have lower conformational degrees of freedom than the analogous saturated compounds. For example, the association constants for the complexation of trans-3-hexenoate and 6-heptenoate with α-CD were approximately half those corresponding to hexanoate and heptanoate (Rekharsky et al., 1997). Comparison of the relevant $\Delta H$ and $\Delta S$ values for these interactions indicates that this effect was entropic in origin (Rekharsky et al., 1997).

Another example of drastic changes in the entropic terms caused by increasing guest flexibility can be seen in the comparison of the complexations of 1-phenylimidazole and 1-benzylimidazole, for which the affinity toward β-CD was 15 times greater for 1-benzylimidazole than for 1-phenylimidazole. This was attributed to an increased freedom resulting of the addition of an extra methylene group (Rekharsky et al., 1995). Similar conclusions were drawn with α-CD complexes of these molecules (Rekharsky et al., 1995). The main source of the large increase in $\Delta G$ for the complexation of 1-benzylimidazole with both α and β-CD is a highly favorable $\Delta S$, which is partly compensated by an unfavorable $\Delta H$ (Rekharsky et al., 1995). These examples clearly demonstrate the decisive role of the guest's flexibility in the stability of CD complexes. Thus, increasing flexibility or degrees of freedom in a guest molecule leads to more favorable complexation entropy, since more of the possible "conformers" can fit properly into the cavity.

## 4. Conclusion

In conclusion, apparent Dtx aqueous solubility has been successfully increased about 5374 times to 9.98 mg mL$^{-1}$ by using Me-β-CD. This represents the highest Dtx aqueous apparent solubility increment ever reported by using conventional CDs. Interestingly, the combination of solubility experiments to circular dichroism, NMR, ITC and molecular docking calculations helped to identify a bivalent sequential binding mechanism, where a Me-β-CD molecule first interacted with both *tert*-butyl and $C_{30}$–$C_{35}$ aromatic groups, then a second Me-β-CD molecule interacted with the $C_{24}$–$C_{29}$ aromatic group. This type of binding is not frequently encountered for interactions between CD derivates and guest molecules and has never been reported before in the literature for Dtx. The results reported in this work constitute useful information for both fundamental and applied pharmacy.

## Acknowledgments

The Association of Cancer Research "ARC" is gratefully acknowledged for the financial support which enabled Ms. Silvia Mazzaferro to conduct this study.

## Appendix A. Supplementary data

Supplementary data associated with this article can be found, in the online version, at doi:10.1016/j.ijpharm.2011.06.034.

## References

Agüeros, M., Ruiz-Gatón, L., Vauthier, C., Bouchemal, K., Espuelas, S., Ponchel, G., Irache, 2009. Combined hydroxypropyl-β-cyclodextrin and poly (anhydride) nanoparticles improve the oral permeability of paclitaxel. Eur. J. Pharm. Sci. 38, 405–413.

Alcaro, S., Ventura, C.A., Paolino, D., Battaglia, D., Ortuso, F., Cattel, L., Puglisi, G., Fresta, M., 2002. Preparation, characterization, molecular modeling and in vitro activity of paclitaxel–cyclodextrin complexes. Bioorg. Med. Chem. Lett. 12, 1637–1641.

Bellocq, N.C., Pun, S.H., Jensen, G.S., Davis, M.E., 2003. Transferrin-containing, cyclodextrin polymer-based particles for tumor-targeted gene delivery. Bioconjug. Chem. 14, 1122–1132.

Bouchemal, K., Couvreur, P., Daoud-Mahammed, S., Poupaert, J., Gref, R., 2009a. A comprehensive study on the inclusion mechanism of benzophenone into supramolecular nanoassemblies prepared using two water-soluble associative polymers. J. Therm. Anal. Calorim. 98, 57–64.

Bouchemal, K., Agnely, F., Koffi, A., Ponchel, G., 2009b. A concise analysis of the effect of temperature and propanediol-1,2 on Pluronic F-127 micellization using isothermal titration microcalorimetry. J. Colloid Interface Sci. 338, 169–176.

Bouchemal, K., 2008. New challenges for pharmaceutical formulations and drug delivery systems characterization using isothermal titration calorimetry. Drug Discov. Today 13, 960–972.

Bouquet, W., Ceelen, W., Fritzinger, B., Pattyn, P., Peeters, M., Remon, J.P., Vervaet, C., 2007. Paclitaxel/b-cyclodextrin complexes for hyperthermic peritoneal perfusion – formulation and stability. Eur. J. Pharm. Biorpharm. 66, 391–397.

Brewster, M.E., Loftsson, T., 2007. Cyclodextrins as pharmaceutical solubilizers. Adv. Drug Deliv. Rev. 59, 645–666.

Daoud-Mahammed, S., Agnihotril, S.A., Bouchemal, K., Klöters, S., Couvreur, P., Gref, R., 2010. Efficient loading and controlled release of benzophenone-3 entrapped into self-assembling nanogels. Curr. Nanosci. 6, 1–12.

Daoud-Mahammed, S., Couvreur, P., Bouchemal, K., Chéron, M., Lebas, G., Amiel, C., Gref, R., 2009. Cyclodextrin and polysaccharide-based nanogels: entrapment of two hydrophobic molecules, benzophenone and tamoxifen. Biomacromolecules 10, 547–554.

Davis, M.E., Brewster, M.E., 2004. Cyclodextrin-based pharmaceutics: past, present and future. Nat. Rev. Drug Discov. 3, 1023–1035.

Del Valle, E.M.M., 2004. Cyclodextrins and their uses: a review. Process Biochem. 39, 1033–1046.

Dordunoo, S.K., Burt, H.M., 1996. Solubility and stability of taxol: effects of buffers and cyclodextrins. Int. J. Pharm. 133, 191–201.

Duchêne, D., Wouessidjewe, D., Ponchel, G., 1999. Cyclodextrins and carrier systems. J. Control. Release 62, 263–268.

Engels, F.K., Verweij, J., 2005. Pharmacokinetic optimization of docetaxel dosing. Eur. J. Cancer 41, 1117–1126.

Fini, P., Castagnolo, M., Catucci, L., Cosma, P., 2004. Inclusion complexes of rose bengal and cyclodextrins. Thermochim. Acta 418, 33–38.

Friesner, R.A., Banks, J.L., Murphy, R.B., Halgren, T.A., Klicic, J.J., Mainz, D.T., Repasky, M.P., Knoll, E.H., Shelley, M., Perry, J.K., Shaw, D.E., Francis, P., Shenkin, P.S.J., 2004. Glide: a new approach for rapid, accurate docking and scoring. 1. Method and assessment of docking accuracy. Med. Chem. 47, 1739–1749.

Hamada, H., Ishihara, K., Masuoka, N., Mikuni, K., Nakajima, N.J., 2006. Enhancement of water-solubility and bioactivity of paclitaxel using modified cyclodextrins. Biosci. Bioeng. 102, 369–371.

Han, S.M., Purdie, N., 1984. Solute induced circular dichroism: complexation of achiral drugs with cyclodextrin. Anal. Chem. 56, 2822–2825.

Higuchi, T., Connor, K., 1965. Phase-solubility techniques. Adv. Anal. Chem. Instrum. 4, 117–212.

Kagkadis, K., 2007. Inclusion complex of taxol with 2-hydroxypropyl-beta-cyclodextrin. US Patent 7,307,176.

Kano, K., Kitagishi, H., Tamura, S., Yamada, A., 2004. Anion binding to a ferric porphyrin complexed with per-O-methylated β-cyclodextrin in aqueous solution. J. Am. Chem. Soc. 126, 15202–15210.

Kikkawa, M., Sablin, E.P., Okada, Y., Yajima, H., Fletterick, R.J., Hirokawa, N., 2001. Switch-based mechanism of kinesin motors. Nature 411, 439–445.

Kleywegt, G.J., 2007. Crystallographic refinement of ligand complexes. Acta Crystallogr. D: Biol. Crystallogr. 63, 94–100.

Lee, S., Seo, D., Kim, H.W., Jung, S., 2001. Investigation of inclusion complexation of paclitaxel by cyclohenicosakis-(1→2)-(β-D-glucopyranosyl), by cyclic-(1→2)-β-D-glucans (cyclosophoraoses), and by cyclomaltoheptaoses (β-cyclodextrins). Carbohydr. Res. 334, 119–126.

Liu, Y., Chen, G.S., Li, L., Zhang, H.Y., Cao, D.X., Yuan, Y.J., 2003. Inclusion complexation and solubilization of paclitaxel by bridged bis(β-cyclodextrin)s containing a tetraethylenepentaamino spacer. J. Med. Chem. 46 (22), 4634–4637.

Liu, Y., Chen, G.S., Chen, Y., Cao, D.X., Ge, Z.Q., Yuan, Y.J., 2004. Inclusion complexes of paclitaxel and oligo (ethylenediamino) bridged bis(β-cyclodextrin)s: solubilization and antitumor activity. Bioorg. Med. Chem. 12, 5767–5775.

Liu, Y., Li, L., Chen, Y., Yu, L., Fan, Z., Ding, F., 2005. Molecular recognition thermodynamics of bile salts by β-cyclodextrin dimers: factors governing the cooperative binding of cyclodextrin dimers. J. Phys. Chem. B 109, 4129–4134.

Loftsson, T., Duchêne, D., 2007. Cyclodextrins and their pharmaceutical applications. Int. J. Pharm. 329, 1–11.

Loftsson, T., Magnusdottir, A., Masson, M., Sigurjonsdottir, J.F., 2002. Self-association and cyclodextrin solubilization of drugs. J. Pharm. Sci. 91, 2307–2316.

López-Nicolás, J.M., Bru, R., Sánchez-Ferrer, A., García-Carmona, F., 1995. Use of soluble lipids' for biochemical processes: linoleic acid-cyclodextrin inclusion complexes in aqueous solution. Biochem. J. 308, 151–154.

Maestrelli, F., González-Rodríguez, M.L., Rabasco, A.M., Ghelardini, C., Mura, P., 2010. New "drug-in cyclodextrin-in deformable liposomes" formulations to improve the therapeutic efficacy of local anaesthetics. Int. J. Pharm. 395, 222–231.

Magnusdottir, A., Masson, M., Loftsson, T., 2002. Self association and cyclodextrin solubilization of NSAIDs. J. Incl. Phenom. Macrocycl. Chem. 44, 213–218.

Mulder, A., Auletta, T., Sartori, A., Del Ciotto, S., Casnati, A., Ungaro, R., Huskens, J., Reinhoudt, D.N., 2004. Divalent binding of a bis(adamantyl)-functionalized calix[4]arene to β-cyclodextrin-based hosts: an experimental and theoretical study on multivalent binding in solution and at self-assembled monolayers. J. Am. Chem. Soc. 126, 6627–6636.

Nogales, E., Wolf, S.G., Downing, K.H., 1998. Structure of the alpha beta tubulin dimer by electron crystallography. Nature 391, 199–203.

Nuijen, B., Bouma, M., Schellens, J., Beijnen, J., 2001. Progress in the development of alternative pharmaceutical formulations of taxanes. Invest. New Drugs 19, 143–153.

Othman, M., Bouchemal, K., Couvreur, P., Gref, R., 2009. Microcalorimetric investigation on the formation of supramolecular nanoassemblies of associative polymers loaded with gadolinium chelate dérivatives. Int. J. Pharm. 379, 218–225.

Othman, M., Bouchemal, K., Couvreur, P., Desmaële, D., Morvan, E., Pouget, T., Gref, R., 2011. A comprehensive study of the spontaneous formation of nanoassemblies in water by a "lock-and-key" interaction between two associative polymers. J. Colloid Interface Sci. 354, 517–527.

Parthier, C., Kleinschmidt, M., Neumann, P., Rudolph, R., Manhart, S., Schlenzig, D., Fanghanel, J., Rahfeld, J.U., Demuth, H.U., Stubbs, M.T., 2007. Crystal structure of the incretin-bound extracellular domain of a G protein-coupled receptor. Proc. Natl. Acad. Sci. U.S.A. 104, 13942–13947.

Perozzo, R., Jelesarov, I., Bosshard, H.R., Folkers, G., Scapozza, L., 2000. Compulsory order of substrate binding to herpes simplex virus type 1 thymidine kinase. J. Biol. Chem. 21, 16139–16145.

Pettersen, E.F., Goddard, T.D., Huang, C.C., Couch, G.S., Greenblatt, D.M., Meng, E.C., Ferrin, T.E., 2004. UCSF Chimera – a visualization system for exploratory research and analysis. J. Comput. Chem. 25, 1605–1612.

Rajewsky, R.A., Stella, V., 1996. Pharmaceutical applications of cyclodextrins. 2. In vivo drug delivery. J. Pharm. Sci. 85 (11), 1142–1169.

Rekharsky, M.V., Goldberg, R.N., Schwarz, F.P., Tewari, Y.B., Ross, P.D., Yamashoji, Y., Inoue, Y., 1995. Thermodynamic and nuclear-magnetic-resonance study of the interactions of alpha-cyclodextrin and beta-cyclodextrin with model substances – phenethylamine, ephedrines, and related substances. J. Am. Chem. Soc. 117, 8830–8840.

Rekharsky, M.V., Mayhew, M.P., Goldberg, R.N., Ross, P.D., Yamashoji, Y., Inoue, Y., 1997. Thermodynamic and nuclear-magnetic-resonance study of the reactions of alpha-cyclodextrin and beta-cyclodextrin with acids, aliphatic-amines, and cyclic alcohols. J. Phys. Chem. 101, 87–100.

Rekharsky, M.V., Inoue, Y., 1998. Complexation thermodynamics of cyclodextrins. Chem. Rev. 98, 1875–1917.

Schmidtchen, F.P., 2002. The anatomy of the energetics of molecular recognition by calorimetry: chiral discrimination of camphor by α-cyclodextrin. Chem. Eur. J. 8, 3522–3529.

Segura-Sanchez, F., Bouchemal, K., Lebas, G., Vauthier, C., Santos-Magalhaes, N., Ponchel, G., 2009. Elucidation of the complexation mechanism between (+)-usnic acid and cyclodextrins studied by isothermal titration calorimetry and phase-solubility diagram experiments. J. Mol. Recognit. 22, 232–241.

Sharma, U.S., Balasubramanian, S.V., Straubinger, R.M., 1995. Pharmaceutical and physical properties of paclitaxel (taxol) complexes with cyclodextrins. J. Pharm. Sci. 84, 1223–1230.

Smith, V.J., Rougier, N.M., de Rossi, R.H., Caira, M.R., Buján, E.I., Fernández, M.A., Bourne, S.A., 2009. Investigation of the inclusion of the herbicide metobromuron in native cyclodextrins by powder X-ray diffraction and isothermal titration calorimetry. Carbohydr. Res. 344, 2388–2393.

Thiele, C., Aurebach, D., Jung, G., Wenz, G., 2010. Inclusion of chemotherapeutic agents in substituted β-cyclodextrin derivatives. J. Incl. Phenom. Macrocycl. Chem. 344, 2388–2393.

Tong, W.-Q., Lach, J.L., Chin, T-Fong., Guilory, J.K., 1991. Microcalorimetric investigation of the complexation between 2-hydroxypropyl-β-cyclodextrin and amine drugs with the diphenylmethyl functionality. J. Pharm. Biomed. 9, 1139–1146.

Vasu Dev, R., Moses Babu, J., Vyas, K., Sai Ram, P., Ramachandra, P., Sekhar, N.M., Mohan Reddy, D.N., Srinivasa Rao, N., 2006. Isolation and characterization of impurities in docetaxel. J. Pharm. Biomed. 40, 614–622.

Werner, T.C., Warner, I.M., 1994. The use of naphthalene fluorescence probes to study the binding sites on cyclodextrin polymers formed from reaction of cyclodextrin monomers with epichlorohydrin. J. Incl. Phenom. Mol. Recog. Chem. 18, 385–396.

Werner, T.C., Colwell, K., Agbaria, R., Warner, I.M., 1996. Binding of pyrene to cyclodextrin polymers. Appl. Spectrosc. 50, 511–516.

Xu, W., Jain, A., Betts, B.A., Demas, J.N., DeGraff, B.A., 2002. Single and multiple binding of β-cyclodextrin and polymeric β-cyclodextrins to luminescent ruthenium(II) α-diimine complexes. J. Phys. Chem. A 106, 251–257.